Hydroquinone clathrate based gas separation (HCBGS): Application to the CO2/CH4 gas mixture

Romuald Coupan, Christophe Dicharry, Jean-Philippe Torre

▶ **To cite this version:**

Romuald Coupan, Christophe Dicharry, Jean-Philippe Torre. Hydroquinone clathrate based gas separation (HCBGS): Application to the CO2/CH4 gas mixture. Fuel, 2018, 226, pp.137-147. 10.1016/j.fuel.2018.03.170 . hal-01985827

HAL Id: hal-01985827
https://hal.science/hal-01985827

Submitted on 18 Jan 2019

HAL is a multi-disciplinary open access archive for the deposit and dissemination of scientific research documents, whether they are published or not. The documents may come from teaching and research institutions in France or abroad, or from public or private research centers.

L'archive ouverte pluridisciplinaire **HAL**, est destinée au dépôt et à la diffusion de documents scientifiques de niveau recherche, publiés ou non, émanant des établissements d'enseignement et de recherche français ou étrangers, des laboratoires publics ou privés.

OATAO
Open Archive Toulouse Archive Ouverte

Open Archive Toulouse Archive Ouverte

OATAO is an open access repository that collects the work of Toulouse researchers and makes it freely available over the web where possible

This is an author's version published in: http://oatao.univ-toulouse.fr/21612

Official URL: https://doi.org/10.1016/j.fuel.2018.03.170

To cite this version:

Coupan, Romuald and Dicharry, Christophe and Torré, Jean-Philippe *Hydroquinone clathrate based gas separation (HCBGS): Application to the CO2/CH4 gas mixture.* (2018) Fuel, 226. 137-147. ISSN 0016-2361

Any correspondence concerning this service should be sent to the repository administrator: tech-oatao@listes-diff.inp-toulouse.fr

Hydroquinone clathrate based gas separation (HCBGS): Application to the CO_2/CH_4 gas mixture

Romuald Coupan, Christophe Dicharry, Jean-Philippe Torré*

CNRS/TOTAL/UNIV PAU & PAYS ADOUR, Laboratoire des Fluides complexes et leurs Réservoirs-IPRA, UMR5150, 64000 PAU, France

Keywords:
CO_2 capture
Hydroquinone
Clathrate
Natural gas treatment
Separation

A B S T R A C T

Hydroquinone (HQ) clathrates have recently been identified as promising candidates for selective gas capture and storage processes. This study evaluates the effectiveness of HQ clathrates in the separation of CO_2 from CO_2/CH_4 gas mixtures, through direct gas/solid reactions in a fixed-bed reactor. The influence of the process operating parameters (i.e. reaction time, pressure, temperature and feed gas composition) on the CO_2 capture kinetics, selectivity towards CO_2, and transient storage capacity were investigated. The experiments were performed using either pure HQ or HQ-based composite materials, with temperatures ranging from about 283 to 343 K, pressures from 3.0 to 9.0 MPa, and CO_2 mole fraction in the gas mixture ranging from 0.2 to 1. The experimental results show that over the range of gas composition investigated, the enclathration reaction is selective to CO_2. This preferential CO_2 capture is enhanced at high CO_2 mole fractions, low temperatures and high pressures. Regarding gas capture kinetics, it was confirmed that the composite material is much more efficient than pure HQ crystals. The CO_2 enclathration rate increases with temperature, pressure and CO_2 fraction in the feed gas. For the first time, the feasibility of such gas separation techniques using HQ clathrates was demonstrated at bench scale.

1. Introduction

Natural gas is the 3rd energy source after coal and oil, according to the International Energy Agency [1]. It is mainly composed of CH_4, but it can also contain other compounds including low molecular weight hydrocarbons (such as ethane, propane, butane, pentane), acid gases (such as CO_2 and H_2S), incondensable gases (N_2 and O_2), and traces of rare gases, mercury and water [2]. Light hydrocarbons (especially CH_4) are the main valuable compounds in natural gases. The other constituents are defined as impurities because of the complications they induce, such as decreasing the gas calorific value, and their operating constraints (e.g. condensation, corrosion and plugging). To respect the required specifications for valorization and commercialization of the natural gas, the removal of these impurities is of paramount importance. As acid gases are generally the most constraining (due to their toxic and corrosive properties) and most abundant, in terms of impurities, a gas sweetening treatment (i.e. removal of CO_2 and H_2S) is required. CO_2 in particular one of main gases contributing to greenhouse effects [3] must be captured and stored (e.g. by injection into an underground reservoir) to curb its concentration from increasing in the atmosphere [4]. Actually, several processes are available for removing CO_2 from natural gas (e.g. chemical absorption using amines, adsorption on porous materials, permeation through membranes, condensation, and cryogenic separation) [4,5] for which the CO_2 recovery rate is high, reaching values > 80%. However, these processes are limited by economic criteria related to energy consumption [5,6]. In this way, alternative techniques for CO_2 gas capture clathrate based technologies being one of them are subjects of great interest.

Gas clathrates are solid state host guest compounds consisting of a network of self associating molecules forming cavities (called “hosts”) in which gas species (called “guests”) can be encaged [7,8]. The combination of host and guest molecules to form clathrates is only possible in appropriate thermodynamic conditions. These inclusion compounds are known to store large amounts of gases such as CO_2, H_2S, CO, SO_2, CH_4 [9], and to be potentially selective to a specific gas present in a mixture [8]. This latter property has motivated many researchers to investigate the potential of clathrates in gas separation. The principle of this concept is based on the simple fact that when a gas clathrate is formed from a gas mixture, one of the constituents (e.g. CO_2 in a CO_2/CH_4 mixture) may be selectively encaged in the solid structure. A clathrate based separation process would thus comprise a clathrate formation step followed by a dissociation step: (i) the formation step leads to a residual vapor and a solid clathrate under equilibrium, both having different gas compositions (e.g. the gas containing a lower CO_2

* Corresponding author.
E-mail address: jean-philippe.torre@univ-pau.fr (J.-P. Torré).

https://doi.org/10.1016/j.fuel.2018.03.170

concentration than the initial gas mixture, and the clathrate a higher one); (ii) the dissociation step: by changing only the thermodynamic conditions (e.g. an increase of temperature, a decrease of pressure, or both), the gaseous molecules contained in the clathrate are released (e.g. producing a CO_2 rich gas mixture). Theoretically, this concept is very attractive, especially when the gas to be treated is already pressurized, such as for production gas. Actually, additional work is truly necessary to demonstrate the feasibility of such separations at larger scale (e.g. using bench and pilot scale apparatuses).

Among the clathrate based processes, the most studied involves gas clathrate hydrates (often simply called gas hydrates), where the host molecules are water molecules associating by hydrogen bonds, generally formed at high pressure (several MPa) and moderately low temperature (close to 273 K) [10]. Accordingly, the hydrate based gas separation (HBGS) process has already attracted widespread interest [11 20]. Nevertheless, although the HBGS process may be economically competitive (as the enclathration precursor is water, and the process can work under pressure), the deployment of the proof of concept to industrial scale is still limited by numerous critical disadvantages: (i) the additional cost of maintaining a relatively low temperature, required in the reactor to form the hydrates; (ii) the slow crystallization rate; (iii) the insufficient capture selectivity, particularly for the CO_2/CH_4 gas mixture; (iv) the necessity to add chemical promoters to overcome the thermodynamic and kinetic limitations [19], some of which can be toxic (e.g. tetrahydrofuran) or cause foaming problems during hydrate dissociation (e.g. sodium dodecyl sulfate); and (v) the operating and technological constraints related to the handling and transport of the multiphase mixture under pressure (i.e. slurry composed by solid hydrates, liquid water, and gases). There are plenty of examples in literature of studies carried out to address these challenges, many of them based on semiclathrates (e.g. TBAB, TBAF, etc.). The main advantage of using these substances is that the HGBS process can be operated at near ambient pressure and/or temperature conditions [20].

Alternatively, hydroquinone (α HQ) is an organic compound from the phenol family, well known to form gas clathrates. Although organic clathrates were discovered over a century ago [21], they were mainly fascinating scientific curiosities, but very few practical applications were proposed to date. A very limited number of studies involving organic clathrates is available in literature, in comparison to common gas hydrates. For example, the precise molecular structure of the simple CO_2 HQ clathrate was reported only recently by Torré et al. [22] showing that much remains to be done even at the fundamental level to increase our understanding of such compounds. The stoichiometry of the HQ clathrate (β HQ) is 3:1 (i.e. 3 molecules of HQ per guest molecule), leading to a maximum storage capacity of 3.03 mol^{Guest}/kg^{HQ} [23]. Recently, Coupan et al. showed that HQ clathrates can be formed with CO_2, CH_4 and CO_2/CH_4 mixtures over a wide range of temperatures (up to about 354 K) and at moderate pressure (< 1 MPa) [24,25]. Moreover, HQ clathrates can form by direct gas solid reaction (i.e. a solvent is not required) by simply contacting solid HQ with the gas in appropriate pressure and temperature conditions [26 28]. As the kinetics of this solid solid transition (i.e. from α to β HQ) is rather slow, an innovative HQ based composite material had already been developed by the authors to primarily improve the enclathration kinetics, as well as to also overcome some process limitations. With the composite: (i) a gas solid enclathration reaction is achieved, for which the induction time (i.e. the waiting period before the α HQ starts to transform into α HQ) is cancelled and the global kinetics is significantly improved; (ii) it permits both enclathration formation and additional adsorption phenomena; (iii) it is compatible with industrial gas solid contactors such as fixed bed reactors; (iv) this composite can be re used over several capture/regeneration cycles; and (v) it avoids the handling of HQ powder, the fine particles to be blown in the process unit, and high pressure drop in the gas/solid contactors [27]. Interestingly, various authors have reported that the HQ clathrates could be used for the selective capture of CO_2 from various CO_2 containing gas mixtures (such as CO_2/H_2, CO_2/N_2 and CO_2/CH_4 gas mixtures) [29 33]. Particularly, Coupan et al. and Lee et al. gave clear evidence on the capability of HQ clathrates in the selective trapping of CO_2 from an equimolar CO_2/CH_4 mixture [32 33]. However, only one quantitative selectivity of 29 mol^{CO2}/mol^{CH4} from the equimolar CO_2/CH_4 mixture has been reported in literature to date, without any precision on the pressure and temperature condition associated to this result [33].

The present work aims at providing a technical performance evaluation of a HQ clathrate based gas separation (denoted as HCBGS in the following) process applied to a CO_2/CH_4 gas mixture. The CO_2/CH_4 gas mixture and the experimental conditions of this study were chosen to approach the industrial case study of the gas sweetening applications [2,34]. The experiments were performed with CO_2/CH_4 gas mixtures with CO_2 mole fraction from 0.2 to 1 in the ~283 343 K and pressure from 3.0 to 9.0 MPa. The CO_2 capture selectivity, the transient gas storage capacity (i.e. the quantity of gas captured at a given time), and the capture kinetics were assessed. The first part of the study was devoted to the use of pure native HQ. Although we believe that the direct use of such crystals is not suitable for industrial purposes, this configuration represents a case study in which the gas capture is due only to enclathration. Therefore, this medium was used to investigate and understand the influence of the process parameters on the separation efficiency. In the second part, an HQ based composite was used for the separation. This conditioning has shown to give better results in terms of kinetics than native HQ crystals, but the phenomena involved in the CO_2 capture are more complex as they involve both adsorption (on the porous medium) and enclathration (with HQ). With this composite, the influence of the process parameters was also analyzed and compared against the native HQ crystals.

2. Experimental section

2.1. materials

HQ (purity of 99.5 mol%) was purchased from Acros Organics. Helium, CO_2 and CO_2/CH_4 gas mixtures (minimum mole fraction purity of 99.995%) were purchased from Linde Gas SA. The CO_2 mole fractions of the CO_2/CH_4 mixtures were measured by chromatography at 0.204, 0.399, 0.501, 0.601, 0.733 and 0.795. These values are in agreement with those given by the supplier specified within a relative uncertainty of ± 2%. The mixtures will be referenced in the following by the nominal values, as 0.20, 0.40, 0.50, 0.60, 0.75 and 0.80.

For the experiments, either native HQ or HQ based composite were used. Native HQ was put in contact with pure CO_2 gas at 3.0 MPa and ambient temperature for 1 month to form CO_2 HQ clathrates, followed by a dissociation step at 1 kPa and 343 K until all the stored gas was released. This process generates a preformed form of HQ with a highly reduced induction time [32]. The structure of the preformed HQ was investigated by Raman spectroscopy just before contacting the CO_2/CH_4 gas mixture (by taking a sample inside the reactor). The analysis revealed the presence of a mixture of α HQ and guest free β HQ, with the α HQ structure in majority (the two HQ forms cannot be dosed precisely with such Raman analysis). Moreover, several other Raman spectroscopic analyses achieved on the cross section of preformed HQ crystals revealed that (in these conditions) the crystals present a core shell structure: the guest free β HQ structure forms the external shell while the crystal core is composed of α HQ.

The HQ based composite used in this work is the one synthesized by Coupan et al. with a dry impregnation process [27]. It consists of Siliasphere® silica particles (size 200 500 μm, pore size of 100 nm, specific area of 57 m^2/g, and porous volume of 0.83 cm^3/g) impregnated with HQ. The HQ content is 0.44 g^{HQ}/g^{Silica}. The composite material was also pre formed with the pure CO_2 in the same conditions as those used for preforming native HQ. As the HQ crystallites are mainly deposited inside the pores of the silica particles, the internal structure of

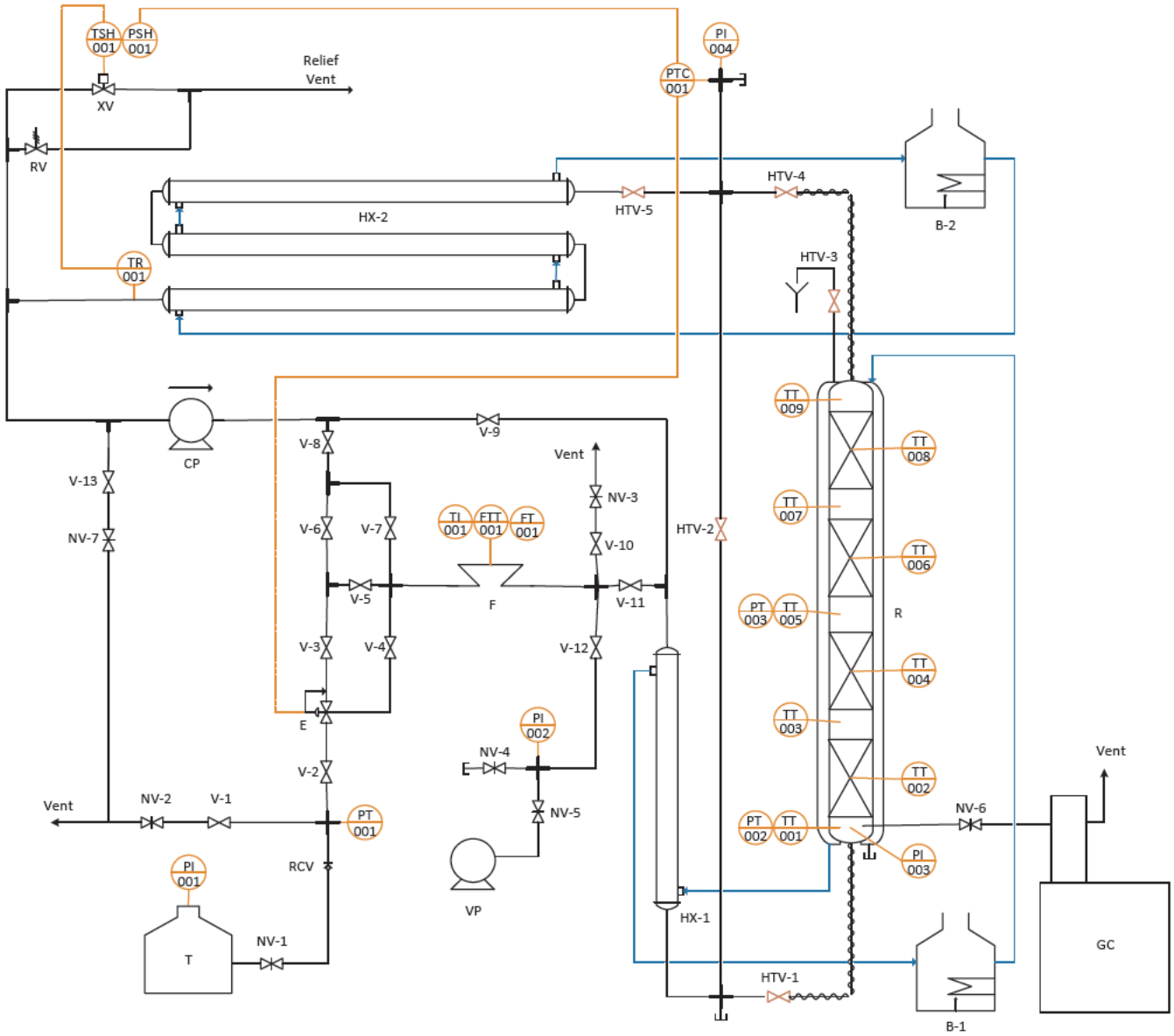

Fig. 1. HCBGS process: (T) gas tank; (E) regulator expander; (CP) gas circulator pump; (VP) vacuum pump; (F) Coriolis flowmeter; (HX) heat exchanger; (R) fixed-bed reactor; (B) thermostatic bath; (GC) gas chromatograph; (V) plug valve; (NV) needle valve; (RCV) rapid connection valve; (HTV) high-temperature plug valve; (RV) relief valve; (XV) pneumatic valve. Blue line refers to heat transfer fluid. (For interpretation of the references to color in this figure legend, the reader is referred to the web version of this article.)

such nanocrystals cannot be investigated as it was not possible to isolate and cut a crystallite with a scalpel to analyze its cross section). Therefore, following our conclusions obtained with native HQ crystals, we assume that the HQ crystals deposited in the composite have a similar core shell structure after the preforming step (i.e. a core of α HQ surrounded by a shell of guest free β HQ).

2.2. Apparatus

The experiments were conducted in an HCBGS process at bench scale. This batch process consists of a closed loop across a fixed bed reactor. The main instruments of the setup are: a regulator expander, a Coriolis flowmeter, a gas circulator pump, a reactor, a gas chromatograph, and two coaxial heat exchangers. Except for the reactor and the chromatograph, the equipment is mounted on a support frame specially designed for the process. A P&ID of the experimental setup is shown in Fig. 1.

The reactor (from NovaSwiss) is a column 1.0 m high with an inner diameter of 25.4 mm, consisting of four removable jacketed sections (each 0.25 m high) made of 316L stainless steel. Five perforated grids are used between each section to prevent particles from flying away. The grids at the inlet and outlet of the reactor have pore sizes of 10 µm, and the intermediate grids have pore sizes of 50 µm. The reactor can run experiments at pressures and temperatures up to 1.5 MPa and 473 K. The temperature is measured by means of nine Pt100 probes (with an accuracy of 0.1 K) placed all along the reactor. The temperature is maintained at the desired value with a stability of ± 0.2 K by continuous forced water circulation in the jacket using a thermostatic bath (Polystat 37, Fischer Scientific). The pressure is measured by three 0–30 MPa Keller model PAA35X sensor transducers (with uncertainties of ± 0.01 MPa), a numerical manometer (model LeoII) and a 0–20 MPa pressure gauge (from Swagelok). Gas sampling is performed through a needle valve located on the reactor. The gas is analyzed by a gas chromatograph which works with a high pressure sampling system (Agilent, model 7820A). It is equipped with a capillary column of 30 m length and 0.32 mm inner diameter, comprising a stationary phase of

polystyrene/di vinylbenzene coating 20 µm thick (model HP PLOT Q) and a thermal conductivity detector. The carrier gas is supplied by a hydrogen generator (model NMH2). The chromatograph is calibrated with different CO_2/CH_4 gas mixtures allowing for quantitative measurements with a 0.3% relative uncertainty. The retention times for CH_4 and CO_2 are 0.64 ± 0.05 and 0.80 ± 0.05 min respectively.

The setup is supplied with feed gas by means of a pressure regulator expander (model ER5000 from TESCOM). The expander works with an N_2 gas flow at 0.6 MPa as the pneumatic supply. The feedback pressure signal comes from the pressure sensor transducer at the reactor head. Gas tanks of variable volume are used to feed the whole system. The pressure at the inlet of the expander is measured by a 0 30 MPa Keller model PA33X sensor transducer (with uncertainties of ± 0.01 MPa). The whole volume placed upstream of the expander is estimated at 994 cm^3. A vacuum pump is used to produce a primary vacuum of 0.1 kPa which is measured by means of a numerical manometer (model LeoII) and a 0 0.1 MPa pressure gauge (from Swagelok). The gas circulator pump (model TFK M1 from Gardner Denver) is used to circulate the gas under pressure in the closed loop to homogenize both its temperature and composition before each chromatographic analysis. The circulation flowrate is adjusted through a voltage regulator. A Coriolis flowmeter (model CMF025H from SERV Instrumentation) checks both the gas flowrate and the amount of gas added to the whole system. Two home made heat exchangers homogenize the gas temperature in the closed loop. The exchangers use water as heat transfer fluid; they consist of double walled pipes with shell outer diameter of 0.02 m and measure 0.5 and 1.5 m in length, respectively. The safety of the HCBGS process is ensured by a relief valve, an electro pneumatic valve, and a safety enclosure.

2.3. Procedure

At the beginning of the experiment, about 200 g of solid reactive medium (native HQ crystals or HQ based composites) is loaded into the reactor, and the thermostatic bath temperature is set to 293 K. When the temperature is stable, the whole system is put under vacuum to remove the air initially present. All valves are open except for the valves connected to the vents or the atmosphere (V 1, V 10, V 13 and NV 4 in Fig. 1). As the reactor is under vacuum, valve V 12 is closed and the vacuum pump turned off. In addition, the by pass valves (V 7, V 9 and HTV 2), the expander exhaust valve V 4, and the valve V 6 are closed. Thanks to the regulator expander, the system is first pressurized by helium at 0.5, 1.5 and 2.5 MPa to determine the accurate volume of the system (i.e. total volume of the piping and the reactor after the loading of the reactive medium). Then, the thermostatic bath temperature is set to the desired value and the system is evacuated by opening the valves connected to the vent, and put again under vacuum as described previously. At this point, the system is pressurized by a CO_2/CH_4 gas mixture at 0.03 MPa per second passing through the Coriolis flowmeter to check the amount of gas added to the system. When the system is at the chosen pressure, valve V 3 is closed, the expander is turned off and V 6 is opened. In addition to the flowmeter measurement, the amount of gas added to the system is determined from Eq. (1):

$$n_{gas}|_t^0 = \frac{PV}{zR(T + \Delta T)} \quad (1)$$

where z is the compressibility factor (calculated using the Soave Redlich Kwong equation of state and the van der Waals mixing rules with a binary interaction parameter set to 0.1) [35], P is the pressure of the system, T the temperature, V the volume of the gas phase, and ΔT the temperature increase due to exothermic effect related to gas loading. The relative deviation between the two determinations of the initial gas amount (i.e. from the flowmeter and the equation of state) is about 5%.

For the isothermal condition of capture, the pressure of the system is tracked as a function of time. The pressure decrease (point A to B in Fig. 2) is due to gas capture by the reactive medium (either native HQ or HQ based composite). The time for the capture step is set to 96 h (4 days). During the capture step, the gas phase is sampled and analyzed by chromatography as shown in Fig. 3. Before each gas composition analysis, the gas is homogenized by the circulator pump.

These measurements allow determine, by mass balance, the amount of gas enclosed in the clathrate and its composition. Indeed, the decrease in the molar quantity of the gas phase corresponds to the molar quantity of gas enclosed in the medium. This amount of gas is given by Eq. (2):

$$n^i_{medium}|_t = n^i_{gas}|_t{}^0 - n^i_{gas}|_t = \left.\frac{y^i PV}{zR(T + \Delta T)}\right|_0 - \left.\frac{y^i PV}{zRT}\right|_t \quad (2)$$

where superscript i corresponds to constituent CO_2 or CH_4, y^i is the molar composition of constituent i in the gas mixture. The CO_2 mole fraction in the stored gas (x^{CO2}), the main determined criterion, can be obtained by the ratio of the amount of stored CO_2 to the total amount of stored gas.

To take into consideration a process point of view, three other criteria are evaluated: (i) the separation factor ($S.F.^{CO2/CH4}$), (ii) the CO_2 recovery fraction ($R.F.^{CO2}$), and (iii) the transient storage capacity (q). The latter criterion is the ratio of the amount of gas stored in the clathrate (given by Eq. (2)) to the initial mass of reactive medium.

$S.F.^{CO2/CH4}$, which describes the CO_2 capture selectivity, considers the composition of the stored gas in equilibrium with the gas phase. The higher $S.F.^{CO2/CH4}$, the better the CO_2 separation. This parameter is calculated by Eq. (3):

$$S.F.^{CO2/CH4}|_t = \left.\frac{x^{CO2}/1 - x^{CO2}}{y^{CO2}1 - y^{CO2}}\right|_t \quad (3)$$

where x^{CO2} and y^{CO2} are the CO_2 molar compositions in the CO_2/CH_4 gas mixture at time t in the gas stored in the medium and in the gas phase, respectively. $R.F.^{CO2}$, which gives the proportion of CO_2 recovered from the gas mixture initially loaded in the reactor, is obtained by Eq. (4):

$$R.F.^{CO2}|_t = 1 - \frac{y^{CO2}.\, n_{gas}|_t}{y^{CO2}.\, n_{gas}|_t{}^0} \quad (4)$$

For the release step, the system is first depressurized down to 0.1 MPa through the vent (Fig. 2 from point B to C): valve V 11 is closed and valves V 10 and NV 3 are opened (see Fig. 1). The system is then put under vacuum: valves NV 3 and V 10 are closed, valves V 12 and NV 5 are opened, and the vacuum pump is turned on. Once the primary vacuum is reached, valves V 12 and NV 5 are closed, the vacuum pump is turned off, and the thermostatic bath temperature is set to 343 K. The operating conditions of the release step are set to insure the dissociation of the HQ clathrates in agreement with literature data [32]. At this point, the pressure of the system slowly increases due to the gas released by the reactive medium until it reaches a constant value (Fig. 2, point D). The composition of the released gas is determined by gas chromatography. The system is again depressurized down to vacuum for further release, followed by composition measurements (if the reactive medium has captured enough gas to do this). The release step is completed when the pressure remains invariant over time at a value close to 1 kPa (i.e. primary vacuum) (Fig. 2, point E). During the release step, the composition of the analyzed gas corresponds to the composition of the stored gas. The relative deviation of the mass balance calculated between the capture and release step is less than 1%.

In the experiments, the uncertainties were estimated considering the accuracy of the sensors, the measures of dispersion, and the experimental reproducibility calculated by performing two runs at 293 K/3.0 MPa using the equimolar CO_2/CH_4 gas mixture.

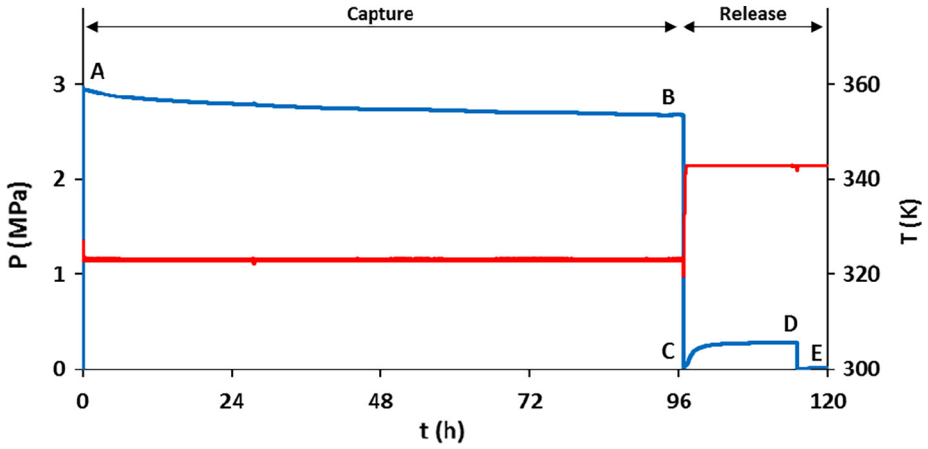

Fig. 2. Example for the capture/release experiment by the HCBGS process loaded with native HQ: system pressure (blue line), and temperature (red line) as a function of time. (For interpretation of the references to color in this figure legend, the reader is referred to the web version of this article.)

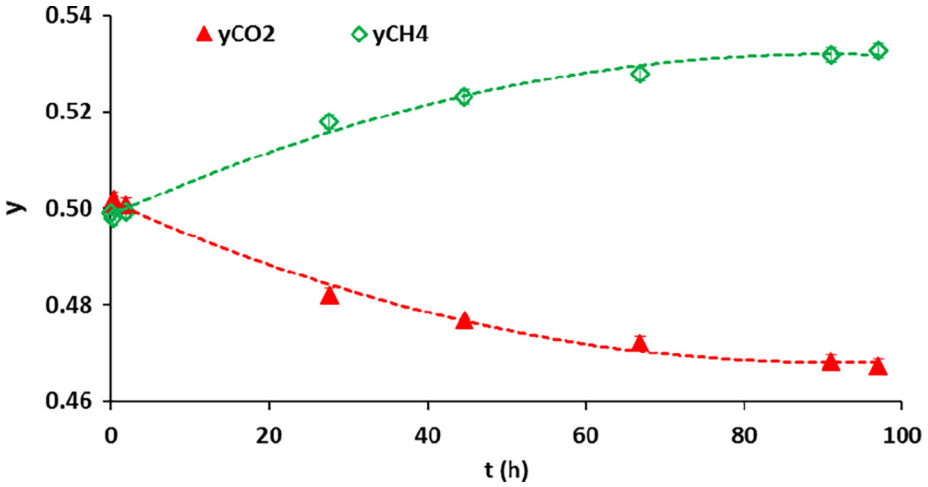

Fig. 3. Example for the capture/release experiment by the HCBGS process loaded with native HQ: CO_2 mole fraction (red line) and CH_4 mole fraction (green line) as a function of time. (For interpretation of the references to color in this figure legend, the reader is referred to the web version of this article.)

3. Results and discussion

3.1. Evaluation of native HQ

First, for each experiment, x^{CO2}, $S.F.^{CO2/CH4}$, $R.F.^{CO2}$ and q are tracked as a function of time to assess the reaction progress. Fig. 4 shows an example of this tracking from the equimolar CO_2/CH_4 gas mixture at 323 K and 3.0 MPa. Note that this trend was observed for all pressure and temperature conditions investigated with the native HQ. Using this reactive medium, it appears that the x^{CO2} stabilizes at a value

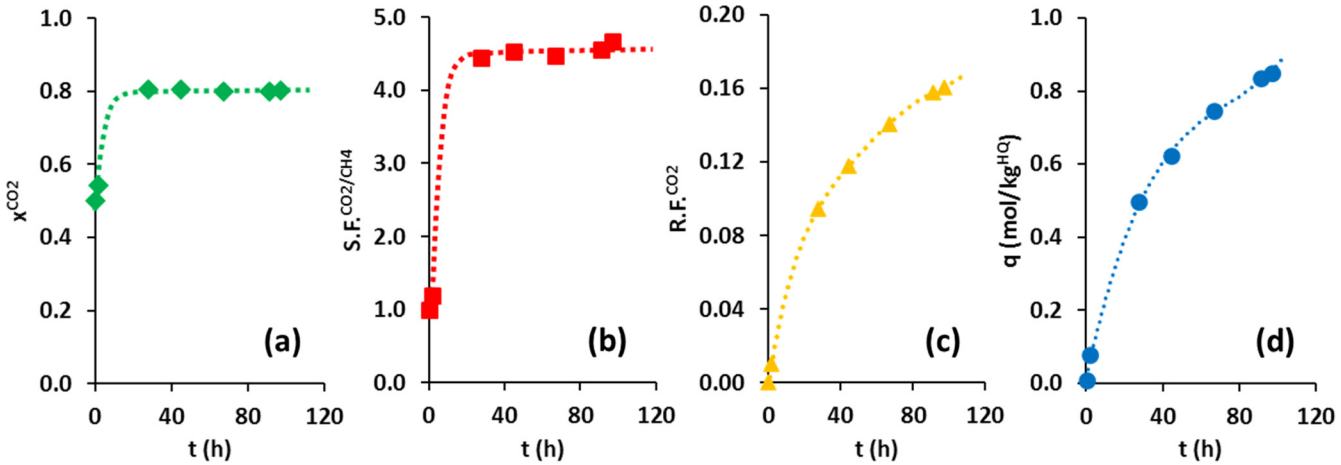

Fig. 4. Experimental curves of native HQ capturing CO_2 from an equimolar CO_2/CH_4 gas mixture at 323 K and 3.0 MPa: (a) CO_2 mole fraction in the stored gas, (b) CO_2 capture selectivity, (c) CO_2 recovery fraction, (d) transient gas storage capacity as a function of time.

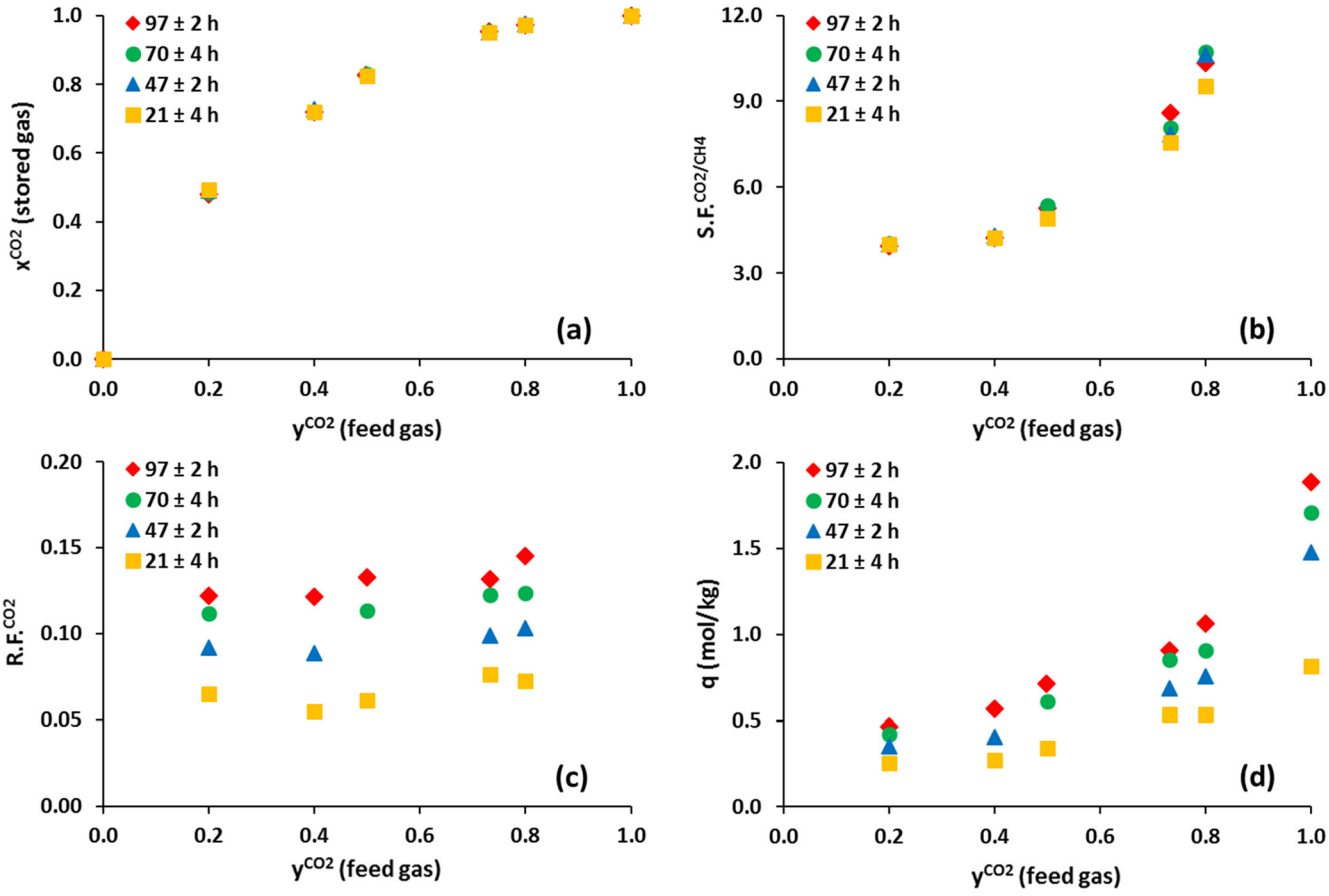

Fig. 5. Experimental curves of native HQ capturing CO_2 from different CO_2/CH_4 gas mixtures at 323 K and 3.0 MPa: (a) CO_2 mole fraction in the clathrate, (b) CO_2 capture selectivity, (c) CO_2 recovery fraction, and (d) transient gas storage capacity. (■) 21 ± 4 h, (▲) 47 ± 2 h, (●) 70 ± 4 h, and (◆) 97 ± 2 h.

of 0.81 in less than 24 h (Fig. 4 a). Therefore, after a transient period (shorter than 24 h), the preferential gas capture phenomenon by HQ is not a time dependent process. In the same way, after the first day of reaction, the $S.F.^{CO2/CH4}$ is almost time independent (Fig. 4 b), as the composition of the gas phase does not change much (i.e. decrease of the CO_2 mole fraction of the gas mixture less than 6%). As the enclathration reaction is not conducted until the full conversion and equilibrium of HQ, the variations of the $R.F.^{CO2}$ (Fig. 4 c) and the q (Fig. 4 d) over time are directly linked to the duration of the experiment and are representative to the enclathration kinetics.

The effects of the feed gas composition and of the pressure and temperature conditions are then assessed. All the numerical values are given in Table S1, in Supplementary material. The experiments are performed with the different CO_2/CH_4 gas mixtures at 293 and 323 K for pressures of 3.0, 6.0 and 9.0 MPa. The release step is not discussed in this part, as the x^{CO2} measured during this step is found to be comparable, to within 0.1%, to the one determined in the capture step.

To begin with, we verified the influence of the feed gas composition on the gas capture. Fig. 5 presents x^{CO2}, $S.F.^{CO2/CH4}$, $R.F.^{CO2}$ and q for the different CO_2/CH_4 gas mixtures. In agreement with the previous discussion concerning the time dependence of these criteria, a global trend is observed for all investigated CO_2/CH_4 gas mixtures: whatever the initial feed gas composition, the preferential capture of CO_2 by native HQ is not time dependent after the first day of reaction (Fig. 5 a). We observed that both the x^{CO2} and the $S.F.^{CO2/CH4}$ increase with the CO_2 mole fraction in the feed gas (Fig. 5 a, b). Indeed, within the range of compositions investigated at 3.0 MPa and 323 K, the selectivity varies from 3.7 to 10.6. Furthermore, these data indicate that the HQ always preferentially capture the CO_2 contained in the CO_2/CH_4 mixtures (i.e. the selectivity is higher than 1) in the entire range of the initial gas composition. Regarding $R.F.^{CO2}$ and q (Fig. 5 c, d), these criteria increase with the CO_2 mole fraction in the feed gas. Effectively, after the 4 day reaction with feed gas containing 0.2 0.8 of CO_2 mole fraction, $R.F.^{CO2}$ increases from 0.12 to 0.14 and q increases from 0.41 to 0.98 mol/kg. Moreover, comparing the latter values against that obtained for a 4 day experiment in the same pressure and temperature conditions with pure CO_2 at about 1.76 mol/kg (Fig. 5 d), we can infer that the presence of CH_4 in the mixture significantly impedes the capture kinetics. These observations confirm that the gas capture kinetics is enhanced for high CO_2 mole fractions, as already reported in literature [32].

Hereafter, we consider the criteria obtained for different pressure and temperature conditions after the 4 day reaction (Fig. 6). The experiments were performed at 293 K over the entire range of the feed gas composition, reaching higher $S.F.^{CO2/CH4}$ values than at 323 K (Fig. 6 a, b). The selectivity varies from 10.1 to 18.8 at 293 K, instead of from 3.7 to 10.6 at 323 K. In the reaction between native HQ and the equimolar CO_2/CH_4 gas mixture (Fig. 6 c, d), x^{CO2} and $S.F.^{CO2/CH4}$ increase at high pressure. When the pressure rises from 3.0 to 9.0 MPa, the selectivity increases from 5.2 to 13.3 at 323 K, and from 15.3 to 19.9 at 293 K. It is worth noting that the impact of temperature is more important than that of pressure: from 3.0 MPa and 323 K, the decrease of 30 K (from 323 to 293 K) increases the $S.F.^{CO2/CH4}$ by a factor of 3, whereas the pressure increase of 6.0 MPa (from 3.0 to 9.0 MPa) increases $S.F.^{CO2/CH4}$ by a factor of 2. Therefore, the preferential capture of CO_2 is enhanced at low temperature, high pressure and for mixtures having high CO_2 content.

The q obtained after the 4 day capture experiments are presented in Fig. 7. Here, we do not consider the $R.F.^{CO2}$ for the comparative purpose, as the whole volume is not the same between the experiments at

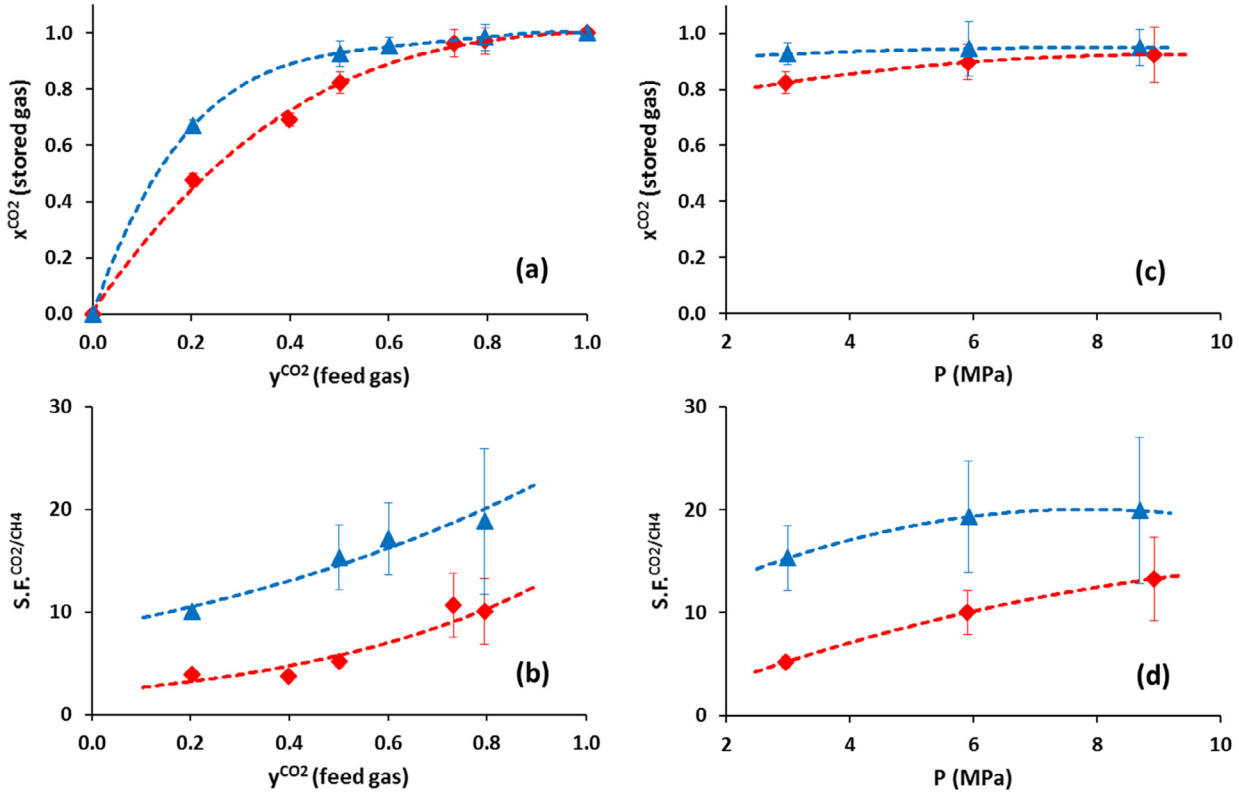

Fig. 6. 4-day capture experiments with native HQ at (blue line) 293 K and (red line) 323 K: (left row) for different CO_2/CH_4 gas mixture at 3.0 MPa, and (right row) for the equimolar CO_2/CH_4 gas mixture at 3.0, 6.0 and 9.0 MPa. (a, c) CO_2 mole fraction in the clathrate, (b, d) CO_2 capture selectivity. (For interpretation of the references to color in this figure legend, the reader is referred to the web version of this article.)

293 and 323 K (i.e. 677 ± 14 cm^3 and 723 ± 15 cm^3 for the experiments at 293 and 323 K respectively) due to the replacement of the reactive medium in the reactor. Note that the medium used for the experiments comes from the same batch of HQ. The change in gas volume is related to the amount of medium loaded into the reactor which can differ slightly from one experiment to another. Fig. 7 a clearly shows that the kinetics is enhanced for mixture having high CO_2 content whatever the temperature (i.e. 293 or 323 K). As an example, after the 4 day reaction at 293 K and 3.0 MPa, it is found 0.30 ± 0.01 mol/kg for a feed gas mixture having a CO_2 mole fraction of 0.2, whereas the transient capacity is 0.79 ± 0.04 mol/kg for a feed gas mixture having a CO_2 mole fraction of 0.8. Moreover, from Fig. 7 b, the transient gas storage capacity increases with the pressure. Indeed, by increasing the pressure by 6.0 MPa (experiments at 3.0 and 9.0 MPa), the q measured increases by about 50% after the 4 day experiments. The kinetics is thus improved at high pressure, which is in agreement with other studies [36]. However, it is worth noting that any increase above 6.0 MPa (e.g. from 6.0 to 9.0 MPa) has no significant impact on q. It is possible that the increase in transient capacity related to the enhancement of gas capture kinetics with pressure is affected by a reduction in clathrate occupancy at high pressure as observed in literature [37]. Now, regarding the effect of temperature, we perceive that the high temperature slightly enhances the kinetics in agreement with literature data [30]. Interestingly, it can be observed that the variation in temperature has an opposite effect on some of the parameters evaluated in this work: whereas high temperature enhances the enclathration kinetics (and thus the quantity of stored gas during the 4 day experiments), it is detrimental for selectivity (which is enhanced at low temperature).

For the operating point at 293 K and 3.0 MPa, the HCBGS process was conceptualized by means of the McCabe Thiele graphical method

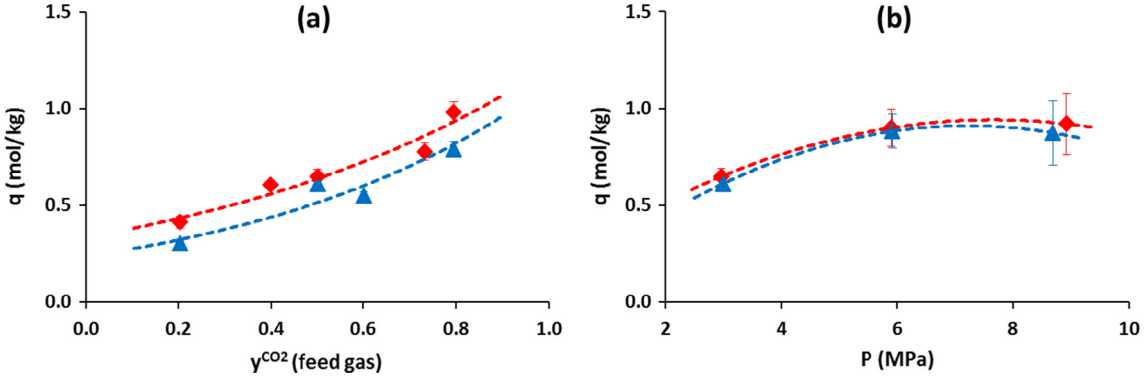

Fig. 7. Transient gas storage capacity after 4 days of reaction between native HQ at 293 K (blue line) and at 323 K (red line) and either (a) different CO_2/CH_4 gas mixtures at 3.0 MPa, or (b) the equimolar CO_2/CH_4 gas mixture at 3.0, 6.0 and 9.0 MPa. (For interpretation of the references to color in this figure legend, the reader is referred to the web version of this article.)

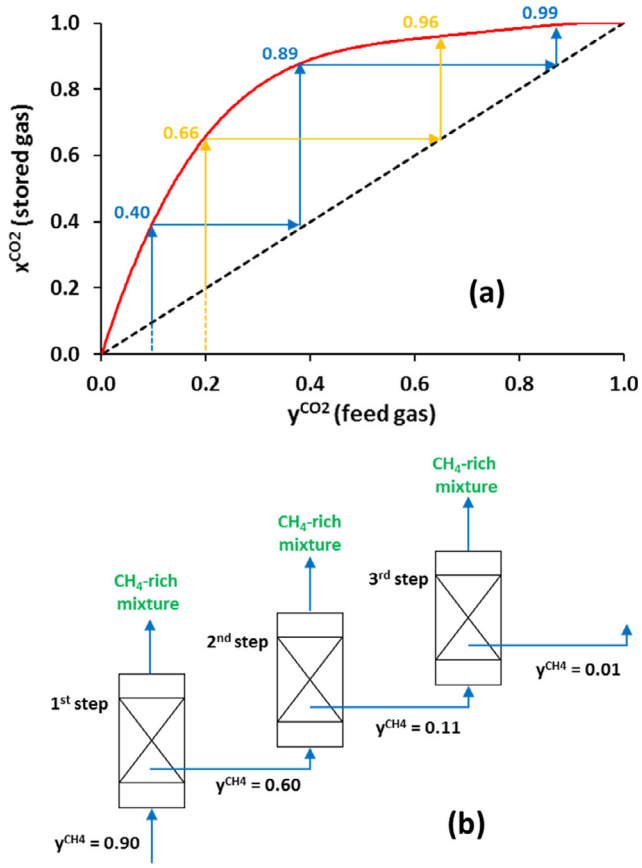

Fig. 8. Conceptual HCBGS process. (a) McCabe-Thiele graphical method: (red line) CO_2 mole fraction in the clathrates as a function of CO_2 mole fraction in the feed gas at 293 K and 3.0 MPa, and (dotted line) x = y line. (b) Schematic diagram of a three-stage HCBGS process at 293 K and 3.0 MPa. (For interpretation of the references to color in this figure legend, the reader is referred to the web version of this article.)

(Fig. 8). The experimental results are used in a polynomial fit to represent the CO_2 mole fraction in the clathrates as a function of CO_2 mole fraction in the feed gas. As our study is directly related to gas sweetening, we illustrate the HCBGS process through two realistic examples using feed gases with a CO_2 mole fraction of 0.2 and 0.1. It thus appears that the CO_2 mole fractions of the CO_2/CH_4 gas mixtures can be concentrated to 0.96 and 0.89 through a two stage HCBGS process from feed gases with a CO_2 mole fraction of 0.2 and 0.1, respectively. Furthermore, a third stage could enrich the recovered mixture to almost pure CO_2 (i.e. CO_2 mole fraction of the CO_2/CH_4 gas mixture of 0.99).

3.2. Evaluation of the HQ based composite

Now considering the HQ based composite, we first investigated the adsorption properties of the native silica support, as the composite is known for combining both adsorption on silica and enclathration by HQ [27]. Table 1 gives the quantity of gas adsorbed and the selectivity obtained for the adsorption of the equimolar CO_2/CH_4 gas mixture at 283, 293, 323 and 343 K for 3.0 and 6.0 MPa on native silica particles.

In all the investigated conditions, the quantity of gas adsorbed on the silica particles is very low (at most 0.16 ± 0.04 mol/kg at 283 K and 6.0 MPa): this represents between 1.3 and 5.2% of the maximum gas storage capacity of the HQ clathrates (i.e. 3.03 mol/kg^{HQ}). This trend is effectively in line with the high pore size (i.e. macro pores of 100 nm) and the low specific area (i.e. specific area of 57 m^2/g) of these particles. However, as for the CO_2 capture selectivity by native silica, it is clear that CO_2 is preferentially adsorbed on this medium in all the tested pressure and temperature conditions (i.e. $S.F.^{CO2/CH4} > 1$). Moreover, we observed that the selectivity is higher at low temperature, and considering the uncertainties, it is probable that selectivity remains unchanged for the investigated pressures. The general trend known for adsorption capacity on silica is observed: enhancement at high pressure and low temperature [38 39].

Table 1
Quantity of gas adsorbed and selectivity of SiliaSphere® silica particles in contact with an equimolar CO_2/CH_4 gas mixture.

P (MPa)	T (K)	q_{ads} (mol/kg)	$S.F.^{CO2/CH4}$
3.00 ± 0.02	283.2 ± 0.2	0.11 ± 0.03	32 ± 17
3.00 ± 0.02	293.2 ± 0.2	0.08 ± 0.02	28 ± 14
3.00 ± 0.02	323.2 ± 0.3	0.06 ± 0.02	6 ± 2
2.99 ± 0.02	343.2 ± 0.3	0.04 ± 0.03	2 ± 1
5.99 ± 0.02	283.2 ± 0.2	0.16 ± 0.04	39 ± 20
6.00 ± 0.02	293.2 ± 0.2	0.15 ± 0.04	9 ± 5
6.00 ± 0.02	323.2 ± 0.3	0.08 ± 0.02	6 ± 3
6.03 ± 0.02	343.2 ± 0.3	0.06 ± 0.02	3 ± 2

From measurements involving the HQ based composite (Fig. 9), we observe that x^{CO2} decreases versus time, as does $S.F.^{CO2/CH4}$ (Fig. 9 a, b). These observations indicate that initially there is a fast, strong capture of CO_2 molecules followed by a second capture that is less CO_2 selective and slower than the first. The fall in the selectivity over time cannot be explained by the two successive phenomena of adsorption on silica and enclathration by HQ. Indeed, the selectivity is about 22 at the start of the experiment for the HQ based composite at 323 K and 3.0 MPa, whereas the native silica achieves a selectivity of 6 in the same conditions. However, as discussed previously in the section on "Materials", we believe that after the dissociation step, most of the HQ crystals have a core shell structure composed of a core of preformed α HQ surrounded by a shell of guest free β HQ. We have already demonstrated in a previous study that the HQ guest free structure formed with CO_2 is much more selective to CO_2 than preformed α HQ [32]. Accordingly, the highest selectivity values measured with the composite just after contacting the gas mixture to HQ could be explained by the presence of the guest free β HQ structure. As the contact area of the impregnated HQ (i.e. crystallites sized 100 nm at most) is much higher than that of native HQ, it would be expected to contain a greater proportion of guest free β HQ and thus have a greater effect on selectivity in the HQ based composite. We believe that the same gas capture mechanisms by enclathration through HQ [32] occur both with the native crystals and with the composite. Nevertheless, as the proportion of guest free structures is supposed to be much higher in the composite than in the native HQ crystals (proportional to the surface to volume ratio of the HQ in the two reactive media), the effects on selectivity are much more visible when the composite is used.

Additionally, Fig. 9 b shows that after 4 days of reaction, the selectivity appears slightly higher for the HQ based composite in comparison to pure HQ. This is logical as the composite allows coupling of the adsorption on silica, filling of the guest free β HQ, and capture by α HQ, in which the first two phenomena are more CO_2 selective than typical enclathration from native HQ. Interestingly, such result suggests that different HQ clathrates may coexist: the final state is composed of CO_2 rich clathrates (obtained from the guest free) and HQ clathrates containing a lower quantity of CO_2 (obtained from the α HQ).

Now, as regarding $R.F.^{CO2}$ (Fig. 9 c), it is obvious that more CO_2 can be recovered from the gas phase by the HQ based composite compared against the native HQ. Indeed, the composite doubles the $R.F.^{CO2}$. Moreover, the quantity of gas captured by the impregnated HQ from the composite materials (i.e. transient gas storage capacity of the clathrate) is found to be higher than that of the native HQ after the 4 day reaction (Fig. 9 d). This confirms that the composite material greatly improves the enclathration kinetics [26]. Nevertheless, it is worth noting (e.g. for scaling up the process) that due to the high

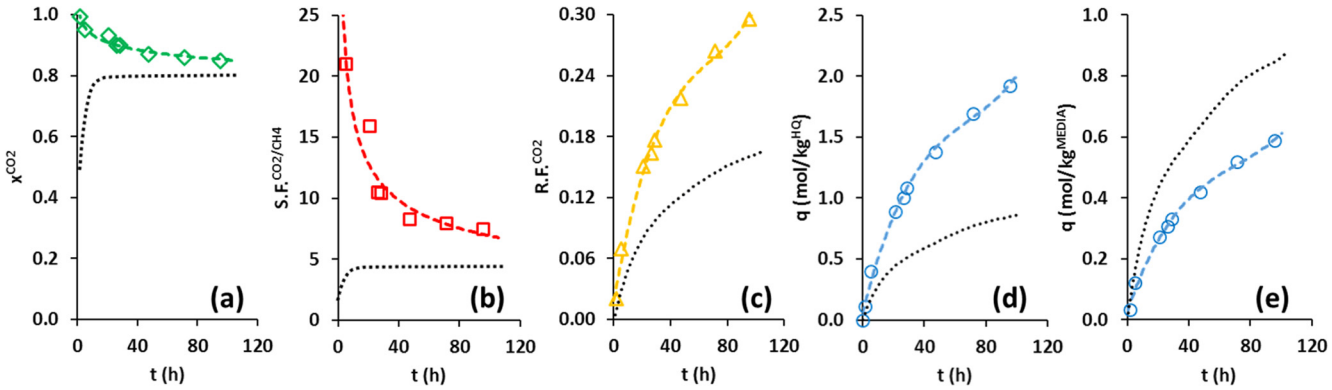

Fig. 9. Experimental curves of CO_2 capture by HQ-based composite, from the equimolar CO_2/CH_4 gas mixture at 323 K and 3.0 MPa: (a) CO_2 mole fraction in the stored gas, (b) CO_2 capture selectivity, (c) CO_2 recovery fraction, (d) transient gas storage capacity of the clathrate, (e) transient gas storage capacity of the media, as a function of time. Black dotted lines represent the values obtained for native HQ in the same pressure and temperature conditions.

proportion of silica in the composite material, the transient global storage capacity of this medium (i.e. molar quantity of CO_2 stored by reference to the mass of the composite) is lower than for native HQ (Fig. 9 e) (e.g. after the 4 day reaction at 323 K and 3.0 MPa, the quantity of gas captured by native HQ is about 20% higher than for the composite material).

The HQ silica composites were then tested in the 4 day capture experiments with the equimolar CO_2/CH_4 gas mixture in the tempera ture range of 283 343 K, and at pressures of 3.0 and 6.0 MPa. x^{CO2}, $S.F.^{CO2/CH4}$, $R.F.^{CO2}$ and q are shown in Fig. 10. All the numerical values are given, for convenience, in Table S2, in Supplementary material. From the evolution of x^{CO2} and $S.F.^{CO2/CH4}$ as a function of temperature (Fig. 10 a, b), the same trend is observed as that previously discussed for native HQ. However, as for the effect of pressure (experiments at 3.0 and 6.0 MPa) and according to the uncertainties, it is worth noting that these parameters have a negligible impact on the selectivity.

Concerning the evolution of $R.F.^{CO2}$ and q as a function of temperature (Fig. 10 c, d), we observed that the maximum value could be reached for temperatures between 293 and 323 K. As the different capture phenomena occurring with the composite materials (i.e. adsorption on silica, filling of the guest free β HQ, and capture by the α HQ) vary in the same way with temperature, the presence of such extrema cannot be linked to them. Therefore, in the temperature range investigated, it appears that both low temperature (< 293 K) and high temperature (> 323 K) have an adverse effect on gas capture by the HQ based composite. However, enclathration being the main phe nomenon, and knowing that the storage capacity of HQ clathrates (at equilibrium) is enhanced at low temperature [24,40], and the capture kinetics is enhanced at high temperature [30], the extremum found on the curves shown in Fig. 10 d for moderate temperature is then lo gical.

The influence of pressure on the recovery fraction (see Fig. 10 c) is in line with the CO_2 capture selectivity, which is somewhat lowered with this parameter. However, the transient storage capacity increases

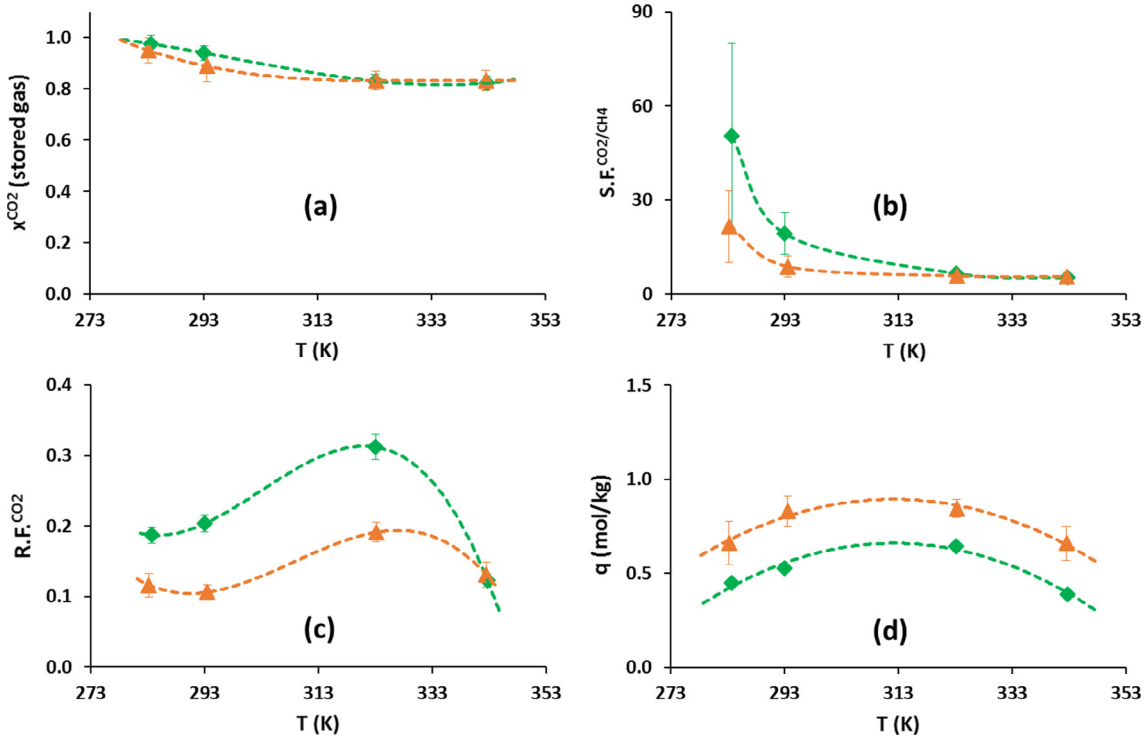

Fig. 10. 4-day capture experiments using HQ-based composite at (green line) 3.0 MPa and (orange line) 6.0 MPa for the equimolar CO_2/CH_4 gas mixture at 283, 293, 323 and 343 K: (a) CO_2 mole fraction in the clathrate, (b) CO_2 capture selectivity, (b) CO_2 recovery fraction, (d) transient gas storage capacity. The volume of the system is 696 ± 25 cm^3. (For interpretation of the references to color in this figure legend, the reader is referred to the web version of this article.)

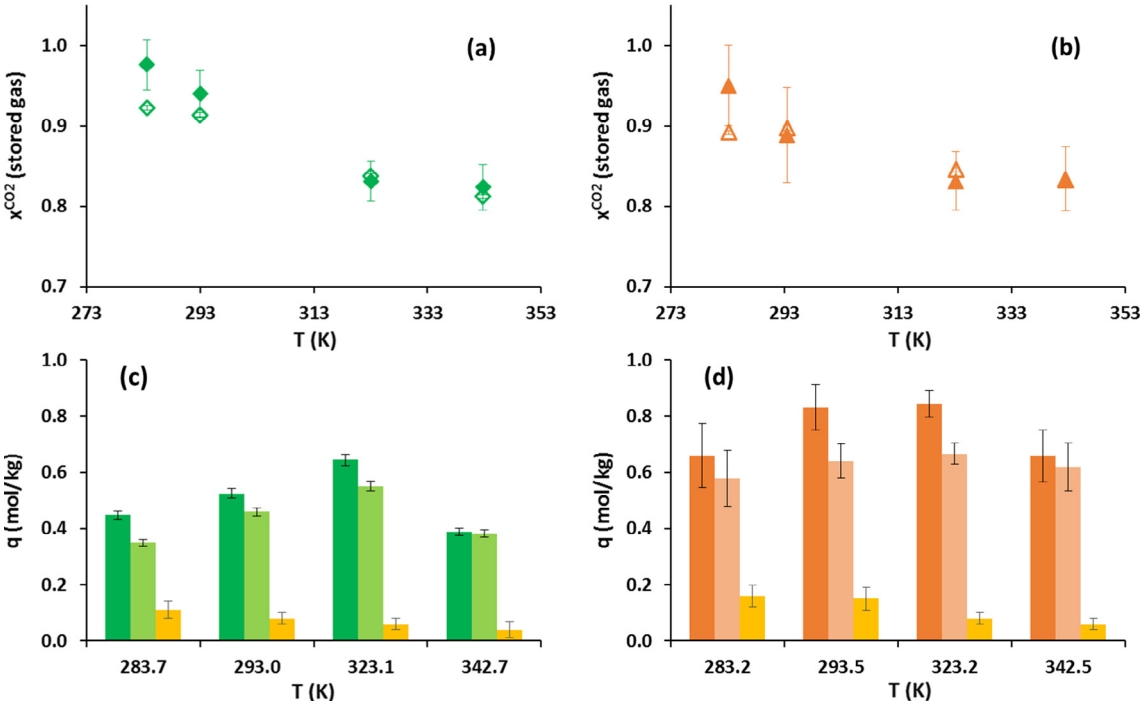

Fig. 11. 4-day capture experiments using HQ-based composite at (a, c) 3.0 MPa and (b, d) 6.0 MPa for the equimolar CO_2/CH_4 gas mixture at 283, 293, 323 and 343 K. (a, b) CO_2 mole fraction of the stored gas: (full symbols) capture step and (open symbols) release step. (c, d) transient gas storage capacity measured: (dark color) capture step, (light color) release step, and (yellow) quantity of gas adsorbed on the native silica particles. (For interpretation of the references to color in this figure legend, the reader is referred to the web version of this article.)

by about 30% when the pressure increases from 3.0 to 6.0 MPa (Fig. 10 d).

When the composite is used, we noted a difference in the mass balance between the gas capture and release steps. As a reminder, in the experimental protocol the release step begins by putting the reactor under vacuum. The gas adsorbed on the support of the composite (i.e. the silica) is evacuated in this step, and cannot be directly measured when the vacuum pump is turned on. Therefore, we assumed that the totality of the gas released after the reactor was put under vacuum is the gas contained in only the HQ clathrates. This assumption is supported by the fact that the clathrate dissociation is rather slow even in vacuum conditions [27,32]. Accordingly, two other parameters that are related only to the HQ clathrates and specific to the release step can be defined and estimated: the CO_2 mole fraction in the clathrates (x_c^{CO2}) and the quantity of gas captured in the clathrate. The results are presented in Fig. 11 and the values are given in Table S2.

For the experiments performed at low temperature, the x_c^{CO2} measured in the release step (Fig. 11 a, b) is found to be generally lower than the x^{CO2} determined in the capture step (e.g. at 283 K, the CO_2 mole fraction are 0.976 ± 0.031 and 0.923 ± 0.003 for the capture and the release step, respectively). However, at high temperature the two values match to within about 1% (e.g. at 323 K, the CO_2 mole fraction values are 0.834 ± 0.080 and 0.833 ± 0.002 for the capture and the release step, respectively). Fig. 11 c, d also presents the transient gas storage capacity determined in both the capture and release steps. As observed, the quantity determined in the capture step is always higher than that in the release step, confirming that adsorption on the support always occurs. Interestingly, the difference between these two determinations is of the same order of magnitude as the quantity of gas adsorbed on the native silica. This is logical, as even though part of the silica surface is covered by HQ crystals in the composite materials, most of the surface is available for adsorption [27]. Therefore, it appears that the HQ based composite materials allow for efficient coupling of adsorption and enclathration: the resulting synergy implies that this medium can be more interesting than both native HQ and native silica.

4. Conclusions

This study presents an assessment of the separation of the CO_2/CH_4 gas mixture through a hydroquinone clathrate based gas separation (HCBGS) process. CO_2 is selectively captured when either native HQ or HQ based composite materials contacts a CO_2/CH_4 gas mixture with a CO_2 mole fraction from 0.2 to 1, in temperatures ranging of 283 343 K and pressures from 3.0 to 9.0 MPa.

Using native HQ, it is demonstrated that the preferential capture of CO_2 molecules is not time dependent after about 24 h, and is enhanced at low temperature, high pressure and for mixtures with a high CO_2 content. After 4 day capture experiments and for all the conditions investigated, the quantity of gas captured in this period (i.e. the transient storage capacity) varies in the same way as selectivity, whereas the gas capture kinetics is enhanced at high temperature, high pressure and for gas mixtures with a high CO_2 content. With the apparatus used and the time interval set for the capture step (4 days in this work), a two stage HCBGS process would be sufficient treating a CO_2/CH_4 gas mixture with a CO_2 mole fraction of at least 0.1, as it is possible to achieve concentrated gas with a CO_2 mole fraction of 0.89.

Concerning the HQ silica composite material, the coupling of adsorption and enclathration phenomena is confirmed. Furthermore, we demonstrated a high CO_2 selective phenomenon occurring at the beginning of the reaction between the composite and the CO_2/CH_4 gas mixtures, attributed to the filling of a substantial amount of guest free β HQ present in the reactive medium. The CO_2 capture selectivity of the composite can thus be preferred over the capture selectivity of either the native HQ or native silica. Moreover, experiments involving the composite confirm that the enclathration kinetic is greatly improved by using this reactive medium. Nevertheless, and despite the kinetics gain, the high proportion of silica contained in HQ based composite materials implies that the global capacity (i.e. molar quantity of CO_2 stored by reference to the mass of the composite) is lower compared to native HQ.

Finally, from a process point of view, the HCBGS process requires certain compromises with the operating parameters, and the three indicators that define the separation efficiency (i.e. the capture selectivity toward CO_2, the kinetics of gas capture, and the transient gas storage capacity of the material used) cannot all be maximized together using a single set of parameters: (i) low temperature conditions insure both high selectivity and high capacity, whereas high temperatures favor the capture kinetics; (ii) the use of an HQ based composite insures high selectivity to CO_2 and enhances the gas capture kinetics, while the global capacity is reduced compared to pure HQ.

Therefore, taking into consideration all the information available on thermodynamics (clathrate formation can be achieved at low pressure and high temperature levels), kinetics (technical solutions are proposed to improve the enclathration rate), and selectivity (preferential capture of CO_2), the HCBGS process could be a valuable alternative to the conventional gas separation processes and may seriously surpass hydrate based technologies for this gas mixture. Additional work is now in progress in our laboratory to evaluate the performance of the HCBGS process for other gas mixtures.

Acknowledgements

Total E&P "Gas Solutions" department, the Carnot Institute ISIFoR (Institute for the Sustainable engIneering of Fossil Resources) and all the working group involved in the ORCHIDS project are acknowledged. Eric Normandin is gratefully acknowledged for the instrumentation of the HCBGS process. Joseph Diaz is also thanked for his technical help.

Author Contributions

The manuscript was written by contributions from all authors. All authors have given approval to the final version of the manuscript.

Funding Sources

The authors would like to thank Total E&P, "Gas Solutions" department for financial support of this work.

Notes

The authors declare no competing financial interest.

Appendix A. Supplementary data

Supplementary data associated with this article can be found, in the online version, at http://dx.doi.org/10.1016/j.fuel.2018.03.170.

References

[1] International Energy Agency. Keys World Energy Statistics; IEA Statistics, OECD Publishing, Paris; 2016.
[2] Lee S, Speight JG, Loyalka SK. Handbook of alternative fuel technologies. 2nd ed. Boca Raton, FL: CRC Press, Taylor & Francis Group; 2015.
[3] Le Quéré C, Andres RJ, Boden T, Conway T, Houghton RA, House JI, et al. The global carbon budget 1959–2011. Earth Syst Sci Data 2013;5:165–85.
[4] Metz B, Davidson O, de Coninck HC, Loos M, Meyer LA. IPCC special report on carbon dioxide capture and storage. Prepared by Working Group III of the intergovernmental panel on climate change. Cambridge, UK: Cambridge University Press; 2005.
[5] Mondal MK, Balsora HK, Varshney P. Progress and trends in CO_2 capture/separation technologies: a review. Energy 2012;46:431–41.
[6] Datta AK, Sen PK. Optimization of membrane unit for removing carbon dioxide from natural gas. J Membr Sci 2006;283:291–300.
[7] Powell HM. The structure of molecular compounds. Part IV. clathrate compounds. J Chem Soc 1948:61–73.
[8] Steed JW, Turner DR, Wallace KJ. Core concepts in supramolecular chemistry and nanochemistry. Chichester, England: John Wiley & Sons; 2007. p. 179–94.
[9] Atwood JL, Davies JED, MacNicol DD. Inclusion compounds, structural aspects of inclusion compounds formed by organic host lattices. vol. 2. London: Academic Press Inc., Ltd.; 1984.
[10] Sloan ED, Koh CA. Clathrate hydrates of natural gases. 3rd ed. Boca Raton: CRC Press, Taylor & Francis Group; 2008.
[11] Linga P, Kumar R, Englezos P. The clathrate hydrate process for post and pre-combustion capture of carbon dioxide. J Hazard Mater 2007;149:625–9.
[12] Babu P, Kumar R, Linga P. Pre-combustion capture of carbon dioxide in a fixed bed reactor using the clathrate hydrate process. Energy 2013;50:364–73.
[13] Babu P, Kumar Linga P. A Review of the hydrate based gas separation (HBGS) process for carbon dioxide pre-combustion capture. Energy 2015;85:261–79.
[14] Denderen MV, Ineke E, Golombok M. CO2 removal from contaminated natural gas mixtures by hydrate formation. Ind Eng Chem Res 2009;48:5802–7.
[15] Ricaurte M, Dicharry C, Broseta D, Renaud X, Torré J-P. CO_2 removal from a CO_2 CH_4 gas mixture by clathrate hydrate formation using THF and SDS as water-soluble hydrate promoters. Ind Eng Chem Res 2013;52:899–910.
[16] Ricaurte M, Dicharry C, Renaud X, Torré J-P. Combination of surfactants and organic compounds for boosting CO_2 separation from natural gas by clathrate hydrate formation. Fuel 2014;122:206–17.
[17] Xia ZM, Li X-S, Chen Z-Y, Lv Q-N, Xu C-G, Chen C. Hydrate-based capture CO_2 and purification CH_4 from simulated landfill gas with synergic additives based on gas solvent. Energy Procedia 2014;61:450–4.
[18] Xia ZM, Li X-S, Chen Z-Y, Li G, Yan K-F, Xu C-G, et al. Hydrate-Based CO_2 Capture and CH_4 Purification from Simulated Biogas with Synergic Additives Based on Gas Solvent. Appl Energy 2016;162:1153–9.
[19] Xu C-G, Yu Y-S, Ding Y-L, Cai J, Li X-S. The effect of hydrate promoters on gas uptake. Phys Chem Chem Phys 2017;19:21769–76.
[20] Zheng J, Zhang P, Linga P. Semiclathrate hydrate process for pre-combustion capture of CO_2 at near ambient temperatures. Appl Energy 2017;194:267–78.
[21] Dyadin YA, Terekhova IS, Rodionova TV, Soldatov DV. Half-century history of clathrate chemistry. J Struct Chem 1999;40:645–53.
[22] Torré J-P, Coupan R, Chabod M, Péré E, Labat S, Khoukh A, et al. CO_2-hydroquinone clathrate: synthesis, purification, characterization and crystal structure. Cryst Growth Des 2016;16:5330–8.
[23] Mak TCW, Lam C-K. Encyclopedia of supramolecular chemistry. In: Atwood JL, Steed JW, editors. vol. 1. Boca Raton, FL: CRC Press, Taylor & Francis Group; 2004. p. 679–86.
[24] Coupan R, Chabod M, Dicharry C, Diaz J, Miqueu C, Torré J-P. Experimental determination of phase equilibria and occupancies for CO_2, CH_4, and N_2 hydroquinone clathrates. J Chem Eng Data 2016;61:2565–72.
[25] Coupan R, Conde MM, Miqueu C, Dicharry C, Torré J-P. Phase equilibrium properties of CO_2/CH_4 mixed gas hydroquinone clathrates: experimental data and model predictions. J Chem Thermodyn 2018;116:230–4.
[26] Lee J-W, Lee Y, Takeya S, Kawamura T, Yamamoto Y, Lee Y-J, et al. Gas-phase synthesis and characterization of CH_4-loaded hydroquinone clathrates. J Phys Chem B 2010;114:3254–8.
[27] Coupan R, Plantier F, Torré J-P, Dicharry C, Sénéchal P, Guerton F, et al. Creating innovative composite materials to enhance the kinetics of CO_2 capture by hydroquinone clathrates. Chem Eng J 2017;325:35–48.
[28] Coupan R, Péré E, Dicharry C, Plantier F, Diaz J, Khoukh A, et al. A characterization study of CO_2, CH_4, and CO_2/CH_4 hydroquinone clathrates formed by gas-solid reaction. J Phys Chem C 2017;121:22883–94.
[29] Lee J-W, Poudel J, Cha M, Yoon SJ, Yoon J-H. Highly selective CO_2 extraction from a mixture of CO_2 and H_2 gases using hydroquinone clathrates. Energy Fuels 2016;30:7604–9.
[30] Lee J-W, Yoon J-H. Preferential occupation of CO_2 molecules in hydroquinone clathrates formed from CO_2/N_2 gas mixtures. J Phys Chem C 2011;115:22647–51.
[31] Lee J-W, Dotel P, Park J, Yoon J-H. Separation of CO_2 from flue gases using hydroquinone clathrate compounds. Korean J Chem Eng 2015;12:2507–11.
[32] Coupan R, Péré E, Dicharry C, Torré J-P. New insights on gas hydroquinone clathrates using in situ Raman spectroscopy: formation/dissociation mechanisms, kinetics and capture selectivity. J Phys Chem A 2017;121:5450–8.
[33] Lee Y-J, Han KW, Jang JS, Jeon T-I, Park J, Kawamura T, et al. Selective CO_2 trapping in guest-free hydroquinone clathrate prepared by gas phase synthesis. Chem Phys Chem 2011;12:1056–9.
[34] Kohl A, Nielsen R. Gas purification. Houston, TX, USA: Gulf Publishing Company; 1997.
[35] Kordas A, Tsoutsouras K, Stamataki S, Tassios D. A generalized correlation for the interaction coefficients of CO_2-hydrocarbon binary mixtures. Fluid Phase Equilib 1994;93:141–66.
[36] Allison SA, Barrer RM. Clathration by phenol and quinol. Part. II kinetics. Trans Far Soc 1968;64:557–65.
[37] Peyronel G, Barbieri G. On some new clathrates of hydroquinone. J Inorg Nucl Chem 1958;8:582–5.
[38] Szekely J, Evans JW, Sohn HY. Gas-solid reactions. New-York, NY, USA: Academic Press Inc.; 1976.
[39] Yang RT. Gas separation by adsorption processes. Stoneham, MA, USA: Butterworth Publishers; 1987.
[40] Conde MM, Torré J-P, Miqueu C. Revisiting the thermodynamic modeling of type I gas-hydroquinone clathrates. Phys Chem Chem Phys 2016;18:10018–27.

Hydroquinone Clathrate based Gas Separation (HCBGS): Application to the CO_2/CH_4 Gas Mixture.

Romuald COUPAN [1], Christophe DICHARRY [1], Jean-Philippe TORRÉ [1,]*

AUTHOR AFFILIATIONS.

1. CNRS/TOTAL/UNIV PAU & PAYS ADOUR, Laboratoire des Fluides complexes et leurs Réservoirs-IPRA, UMR5150, 64000, PAU, France.

* CORRESPONDING AUTHOR: Jean-Philippe TORRE. Address: CNRS/TOTAL/UNIV PAU & PAYS ADOUR, Laboratoire des Fluides complexes et leurs Réservoirs-IPRA, UMR5150, 64000, PAU, France. Tel. +335 40 17 51 09. Email: jean-philippe.torre@univ-pau fr

SUPPLEMENTARY MATERIAL

1. EVALUATION OF THE NATIVE HQ

Table S1. 4-days capture experiments with CO_2/CH_4 gas mixtures and native HQ.

V (cm^3)	P (MPa)	T (K)	y^{CO2} (feed gas)	x^{CO2} (stored gas)	S.F.$^{CO2/CH4}$	R.F.^{CO2}	q (mol/kg)	v^{Gas}(STP)/v^{HQ}
723 ± 15	2.97 ± 0.02	323.2 ± 0.3	0.204 ± 0.001	0.477 ± 0.023	3.9 ± 0.2	0.12 ± 0.01	0.41 ± 0.03	12.0 ± 0.9
723 ± 15	3.01 ± 0.02	323.3 ± 0.3	0.399 ± 0.001	0.692 ± 0.024	3.7 ± 0.2	0.12 ± 0.01	0.61 ± 0.02	17.6 ± 0.7
723 ± 15	2.96 ± 0.02	323.2 ± 0.3	0.501 ± 0.002	0.824 ± 0.040	5.2 ± 0.6	0.13 ± 0.01	0.65 ± 0.04	18.9 ± 1.1
723 ± 15	2.95 ± 0.02	323.2 ± 0.3	0.733 ± 0.002	0.963 ± 0.048	10.1 ± 3.1	0.13 ± 0.01	0.78 ± 0.04	22.7 ± 1.3
723 ± 15	2.97 ± 0.02	323.3 ± 0.3	0.795 ± 0.002	0.972 ± 0.046	10.6 ± 3.2	0.14 ± 0.01	0.98 ± 0.05	28.7 ± 1.5
677 ± 14	2.98 ± 0.02	293.2 ± 0.3	0.204 ± 0.001	0.671 ± 0.020	10.1 ± 0.4	0.23 ± 0.01	0.30 ± 0.01	8.9 ± 0.3
677 ± 14	2.99 ± 0.02	293.2 ± 0.3	0.501 ± 0.002	0.926 ± 0.045	15.3 ± 3.1	0.20 ± 0.02	0.61 ± 0.04	17.8 ± 1.2
677 ± 14	2.99 ± 0.02	293.2 ± 0.3	0.601 ± 0.002	0.955 ± 0.029	17.1 ± 3.5	0.19 ± 0.01	0.55 ± 0.02	16.1 ± 0.5
677 ± 14	2.97 ± 0.02	293.5 ± 0.3	0.795 ± 0.002	0.984 ± 0.046	18.8 ± 7.1	0.16 ± 0.01	0.79 ± 0.04	23.0 ± 1.2
682 ± 14	5.91 ± 0.02	323.1 ± 0.5	0.501 ± 0.002	0.897 ± 0.063	10.0 ± 2.1	0.15 ± 0.02	0.90 ± 0.10	26.2 ± 2.8
682 ± 14	5.92 ± 0.02	293.6 ± 0.3	0.501 ± 0.002	0.945 ± 0.062	19.3 ± 5.4	0.12 ± 0.01	0.88 ± 0.09	25.7 ± 2.6
715 ± 14	8.92 ± 0.03	323.0 ± 0.6	0.501 ± 0.002	0.924 ± 0.098	13.3 ± 4.0	0.10 ± 0.01	0.92 ± 0.16	26.8 ± 4.6
715 ± 14	8.69 ± 0.03	293.5 ± 0.3	0.501 ± 0.002	0.949 ± 0.107	19.9 ± 7.1	0.08 ± 0.01	0.87 ± 0.17	25.5 ± 4.9

2. EVALUATION OF THE HQ-BASED COMPOSITE MATERIALS

Table S2. 4-days capture experiments with the equimolar CO_2/CH_4 gas mixtures and the HQ-based composite. The volume of the system is 696 ± 25 cm^3.

P (MPa)	T (K)	x^{CO2} Capt. step (stored gas)	$S.F.^{CO2/CH4}$	$R.F.^{CO2}$	$q^{Capt. Step}$ (mol/kg)	x^{CO2} Rel. step (stored gas)	$q^{ReL step}$ (mol/kg)
2.99 ± 0.02	283.7 ± 0.4	0.976 ± 0.031	50.5 ± 29.5	0.19 ± 0.01	0.45 ± 0.02	0.923 ± 0.003	0.35 ± 0.01
2.98 ± 0.02	293.0 ± 0.3	0.940 ± 0.029	19.3 ± 6.7	0.20 ± 0.01	0.52 ± 0.02	0.913 ± 0.003	0.46 ± 0.02
3.00 ± 0.02	323.1 ± 0.4	0.831 ± 0.025	6.6 ± 1.0	0.31 ± 0.02	0.64 ± 0.02	0.838 ± 0.003	0.55 ± 0.02
3.02 ± 0.03	342.7 ± 0.8	0.824 ± 0.028	5.2 ± 0.9	0.12 ± 0.01	0.39 ± 0.02	0.812 ± 0.002	0.38 ± 0.01
6.03 ± 0.03	283.2 ± 0.4	0.951 ± 0.050	21.5 ± 11.4	0.12 ± 0.02	0.66 ± 0.11	0.898 ± 0.003	0.58 ± 0.10
5.99 ± 0.02	293.5 ± 0.3	0.889 ± 0.059	8.8 ± 3.4	0.11 ± 0.01	0.83 ± 0.08	0.897 ± 0.003	0.64 ± 0.06
6.05 ± 0.02	323.2 ± 0.4	0.831 ± 0.036	5.8 ± 1.2	0.19 ± 0.01	0.84 ± 0.05	0.846 ± 0.003	0.67 ± 0.03
6.00 ± 0.02	342.5 ± 1.1	0.834 ± 0.040	5.6 ± 1.3	0.13 ± 0.02	0.66 ± 0.09	0.833 ± 0.002	0.62 ± 0.09